

## The E8 lattice and quasicrystals: geometry, number theory and quasicrystals

This article has been downloaded from IOPscience. Please scroll down to see the full text article.

1993 J. Phys. A: Math. Gen. 26 1789

(<http://iopscience.iop.org/0305-4470/26/8/009>)

View [the table of contents for this issue](#), or go to the [journal homepage](#) for more

Download details:

IP Address: 171.66.16.68

The article was downloaded on 01/06/2010 at 21:08

Please note that [terms and conditions apply](#).

# The E8 lattice and quasicrystals: geometry, number theory and quasicrystals

J F Sadoc† and R Mosseri‡

† Laboratoire de physique des solides, batiment 510 F91405-Orsay Cedex, France

‡ Laboratoire de physique des solides de Bellevue, CNRS, F92195-Meudon Cedex, France

Received 6 July 1992

**Abstract.** In this paper we study the quasiperiodic structures which can be derived from E8. This lattice, suitably oriented, leads to a 4D quasicrystal which has  $\{3, 3, 5\}$  symmetry. We develop a modified version of the cut and projection method. The high-dimensional lattice is first foliated into successive shells surrounding a vertex. The shells are embedded into  $\mathcal{D}$   $S^7$  spheres. We then use the so-called Hopf fibration of  $S^7$  to gather families of E8 shell sites into  $S^3$  fibres which contain 24 sites (or a multiple of 24) which are symmetrically disposed in  $S^3$ . This has two advantages: first, in the selection process, a whole fibre is either selected or rejected, which reduces the computation; more importantly, the selection process for a fibre amounts to simple arithmetical criteria. The whole process leads to a shell-by-shell analysis of the 4D quasicrystal, which can be brought onto a 2D–1D algorithm similar to the Fibonacci chain construction. We propose an arithmetic formula which gives the number of points on the shells. This 4D quasicrystal has the interesting feature that it can be sliced into lower-dimensional quasicrystals, for example with icosahedral and tetrahedral symmetry in three dimensions.

## 1. Introduction

A standard method for generating quasiperiodic structures is the cut and projection algorithm (Duneau and Katz 1985, Kalugin *et al* 1985, Elser 1985) which uses higher-dimensional lattices. For example, the 3D icosahedral, 2D five-fold and eight-fold quasiperiodic structures are obtained by mapping, respectively, from 6D, 5D and 4D cubic lattices. An original case was derived by Elser and Sloane (1987), who consider the so called E8 lattice in eight dimensions. E8 is a non-primitive cubic lattice which is part of the root lattice series (Conway and Sloane 1988). The use of root lattices has been extended by Baake *et al* (1990) who considered lattices in the D series. In the context of non-crystalline structures we have shown (Sadoc and Mosseri 1988) that a modified version of the Elser and Sloane (1987) approach allows recovery of the hierarchical polytopes, which were initially introduced for amorphous solids description (Mosseri and Sadoc 1984).

All these polytopes are derived, by decoration, from the  $\{3, 3, 5\}$  polytope which is a template for icosahedral close packed structures. The quasicrystal which is derived from E8 has  $\{3, 3, 5\}$  symmetry, so it could be a useful tool with which to progress the study of non-crystalline close packing. For this reason the quasiperiodic structure is studied in detail, hence developing a modified version of the cut and

projection method. The high-dimensional lattice is first foliated into the successive shells surrounding a vertex. The shells are embedded into  $7D$   $S^7$  spheres. We then use the so-called Hopf fibration of  $S^7$  (section 3 and appendix B) to gather families of E8 shell sites into  $S^3$  fibres which contain 24 sites (or multiples of 24) which are symmetrically disposed in  $S^3$ . This has two advantages: first, in the selection process, a whole fibre is either selected or rejected, which reduces the computation; more importantly, the selection process for a fibre amounts to simple arithmetical criteria. The whole process leads to a shell-by-shell analysis of a 4D quasicrystal (section 4), which can be brought onto a 2D-1D algorithm similar to the Fibonacci chain construction (section 5). A first step towards the determination of explicit coordinates for the quasicrystal sites is given (section 6). This 4D quasicrystal has the interesting feature that it can be sliced into lower-dimensional quasicrystals (section 7), for example with icosahedral and tetrahedral symmetry in three dimensions and with order 5, 12 and 30 in two dimensions.

## 2. The E8 lattice

The E8 lattice provides the densest packing of hard spheres in eight dimensions. This results from its 'laminated' nature, which results in it sometimes being denoted as  $\Lambda_8$ . The laminated lattices  $\Lambda_j$  are the whole series which starts in two dimensions with the triangular lattice. The latter provides the densest packing of circles in two dimensions. Then  $\Lambda_3$  is generated by a suitable stacking of  $\Lambda_2$  in the third dimension.  $\Lambda_3$  is the FCC lattice which also has the densest periodic packing. Stacking FCC lattices in four dimensions leads to  $\Lambda_4$ , also denoted  $\{3,3,4,3\}$ , which is a honeycomb (Coxeter 1973). And so on in higher dimensions, which eventually gives the E8 lattice. An interesting feature of the laminated lattices is their high-density packing fraction which may prove useful for deriving models for quasicrystalline metals.

### 2.1. Description of the lattice

Consider a simple cubic cell in  $R^8$  endowed with the standard orthonormal frame  $e_i$ . The E8 nodes inside this cell are first given by all the permutations of

$$(0^8) \quad \left(\frac{1}{2}^2, 0^6\right) \quad \left(\frac{1}{2}^4, 0^4\right) \quad \left(\frac{1}{2}^6, 0^2\right) \quad \left(\frac{1}{2}^8\right) \quad (2.1)$$

and the above set translated by  $\left(\frac{1}{4}^8\right)$

Written this way E8 bears analogies with the FCC and  $\{3,3,4,3\}$  (where all even-dimensional faces are centred) and even with the diamond structure (two FCC translated by  $\frac{1}{4}$  along the body cube diagonal). The total number of vertices in the cubic cell can be calculated as follow. The number of  $j$ -dimensional faces of an  $n$ -dimensional cube is  $2^{n-j} \binom{n}{j}$  and each such face is shared by  $2^{n-j}$  cells. Hence in the present case half of the vertices are counted by summing  $\binom{8}{j}$  with  $j$  even, which amounts to 128. The second set (translated from the first set along the main diagonal) gives 128 new sites which adds up to 256 sites altogether. Note that this new set occupies the centres of half of the  $2^8$  smaller cubes of length  $\frac{1}{2}$  contained in the unit cube. This is similar to what occurs in the 3D diamond structure.

### 2.2. The first coordination shell

The smallest distance between two nodes is  $\sqrt{2}/2$ . Around the origin these first neighbours are of the type  $(\frac{1}{2}, \frac{1}{2}, 0^6)$  with all signs, which amounts to 112, and also nodes like  $(\frac{1}{4}^8)$ , with the appropriate signs, which gives 128 new neighbours. So the first coordination shell is a semi-regular polytope with 240 vertices, called the Gosset polytope (Coxeter 1973). It bears some analogies to the 3D cuboctahedron. Its 7D faces are 17 280 simplices and 2160 cross polytopes (the latter being equivalent to the octahedron in higher dimension). All smaller dimensional faces are simplices.

### 2.3. The E8 lattice unit cell

Among all possible unit cells (i.e. with one node at the origin and a set of translations which generates the lattice), we shall exhibit two which prove to be interesting. The first set of translation is  $e_i, i = 1, \dots, 8$ :

$$\begin{aligned}
 e_1 &: (\frac{1}{2}, \frac{1}{2}, 0, 0, 0, 0, 0, 0) \\
 e_2 &: (\frac{1}{2}, 0, \frac{1}{2}, 0, 0, 0, 0, 0) \\
 e_3 &: (0, \frac{1}{2}, \frac{1}{2}, 0, 0, 0, 0, 0) \\
 e_4 &: (0, 0, \frac{1}{2}, \frac{1}{2}, 0, 0, 0, 0) \\
 e_5 &: (\frac{1}{4}, \frac{1}{4}, \frac{1}{4}, \frac{1}{4}, \frac{1}{4}, \frac{1}{4}, \frac{1}{4}, \frac{1}{4}) \\
 e_6 &: (\frac{1}{2}, 0, 0, 0, \frac{1}{2}, 0, 0, 0) \\
 e_7 &: (\frac{1}{4}, \frac{1}{4}, \frac{1}{4}, -\frac{1}{4}, \frac{1}{4}, \frac{1}{4}, \frac{1}{4}, -\frac{1}{4}) \\
 e_8 &: (0, \frac{1}{2}, 0, 0, 0, \frac{1}{2}, 0, 0)
 \end{aligned} \tag{2.2}$$

The first three vectors  $e_1, e_2, e_3$  define a rhombus with  $\pi/3$  angles as in the FCC unit cell. The fourth vector  $e_4$  is such that  $e_4 \perp e_1$  and makes a  $\pi/3$  angle with  $e_2$  and  $e_3$ . These first four vectors generate a  $\{3, 3, 4, 3\}$  lattice in  $R^4$ . The last four vectors generate a similar lattice. The second choice for the unit cell is  $f_i, i = 1, \dots, 8$ :

$$\begin{aligned}
 f_1 &: (\frac{1}{2}, \frac{1}{2}, 0, 0, 0, 0, 0, 0) \\
 f_2 &: (\frac{1}{2}, 0, \frac{1}{2}, 0, 0, 0, 0, 0) \\
 f_3 &: (0, \frac{1}{2}, \frac{1}{2}, 0, 0, 0, 0, 0) \\
 f_4 &: (\frac{1}{4}, \frac{1}{4}, \frac{1}{4}, \frac{1}{4}, \frac{1}{4}, \frac{1}{4}, \frac{1}{4}, \frac{1}{4}) \\
 f_5 &: (\frac{1}{4}, \frac{1}{4}, \frac{1}{4}, -\frac{1}{4}, \frac{1}{4}, \frac{1}{4}, \frac{1}{4}, -\frac{1}{4}) \\
 f_6 &: (\frac{1}{4}, \frac{1}{4}, \frac{1}{4}, -\frac{1}{4}, \frac{1}{4}, -\frac{1}{4}, \frac{1}{4}, \frac{1}{4}) \\
 f_7 &: (\frac{1}{4}, \frac{1}{4}, \frac{1}{4}, -\frac{1}{4}, -\frac{1}{4}, \frac{1}{4}, \frac{1}{4}, \frac{1}{4}) \\
 f_8 &: (\frac{1}{4}, \frac{1}{4}, \frac{1}{4}, -\frac{1}{4}, \frac{1}{4}, -\frac{1}{4}, -\frac{1}{4}, \frac{1}{4})
 \end{aligned} \tag{2.3}$$

The eight vectors  $f_i$  point toward the eight vertices of a simplicial cell of the Gosset polytope. All angles at the origin of the cell are  $\pi/3$ ; thus it is a generalization in eight dimensions of the FCC unit cell.

**2.4. A 4D sublattice decomposition**

Similar to the description of a 3D lattice in terms of reticular 2D planes, an 8D lattice can be decomposed into  $n$ -dimensional sublattices, the translation vectors between subspaces defining a complementary  $(8n)$ -dimensional lattice. Here we describe one such decomposition with  $n = 4$ : the  $\{3, 3, 4, 3\}$  reticular lattice (or  $\Lambda_4$ ) which is, for instance, generated by the first four vectors  $e_i, i = 1, \dots, 4$ . In E8 the complementary lattice is also a  $\{3, 3, 4, 3\}$ . This lattice was previously used in the quasicrystal context (Sadoc and Mosseri 1990). Its coordination shell is a  $\{3, 4, 3\}$  polytope (Coxeter 1973), a famous regular self-dual figure with 24 vertices and 24 octahedral cells. The  $\{3, 3, 4, 3\}$  lattice can be viewed both as a face-centred and a body-centred lattice. Indeed it is generated by the simple 4D cubic translations if one decorates the 4D unit cell with the eight nodes

$$\begin{aligned} (0, 0, 0, 0) & \quad (\frac{1}{2}, \frac{1}{2}, 0, 0) & \quad (\frac{1}{2}, 0, \frac{1}{2}, 0) & \quad (\frac{1}{2}, 0, 0, \frac{1}{2}) \\ (0, \frac{1}{2}, 0, \frac{1}{2}) & \quad (0, \frac{1}{2}, \frac{1}{2}, 0) & \quad (0, 0, \frac{1}{2}, \frac{1}{2}) & \quad (\frac{1}{2}, \frac{1}{2}, \frac{1}{2}, \frac{1}{2}). \end{aligned} \tag{2.4}$$

So it is an even-face centred cubic lattice (F). The 3D subspace spanned by the three vectors in (2.4) whose fourth coordinate vanishes contains an FCC lattice, and so does the 3D space defined by  $x_4 = \frac{1}{2}$ . When both lattices are mapped orthogonally (along  $x_4$ ), each node of one lattice falls onto the centre of an octahedral interstice of the other lattice.

Finally, consider the four vectors

$$(\frac{1}{2}, \frac{1}{2}, \frac{1}{2}, \frac{1}{2}) \quad (-\frac{1}{2}, \frac{1}{2}, \frac{1}{2}, -\frac{1}{2}) \quad (-\frac{1}{2}, -\frac{1}{2}, \frac{1}{2}, \frac{1}{2}) \quad (\frac{1}{2}, -\frac{1}{2}, \frac{1}{2}, -\frac{1}{2}) \tag{2.5}$$

which also form an orthonormal basis, and thus define a hypercubic cell. In order to generate all the lattice sites (or vectors) it is necessary to add the  $(0, 0, 1, 0)$  node which is the cell centre. Therefore the  $\{3, 3, 4, 3\}$  lattice can be viewed as a body-centred hypercubic lattice (I).

**3. Hopf fibration of the E8 coordination polytope**

The 240 vertices of the Gosset polytope can be seen as being inscribed in a 7D hypersphere  $S^7$ . As will become clear below, it is interesting to split these 240 vertices into ten equivalent subsets, each belonging to a 3D hypersphere  $S^3$  which does not intersect the nine others. This is nothing other than taking a discrete version of the Hopf fibration of  $S^7$  with fibres  $S^3$  and base  $S^4$ .

We shall use quaternions, the main properties of which are recalled in appendix A, and we follow the presentation by Manton (1987) of the discrete Hopf fibration, which is presented in appendix B.

Let us take the T group elements defined in appendix A, rescaled so as to belong to a sphere  $S^3$  of radius  $\frac{1}{2}$ , forming a new set called  $T_1$ :

$$T_1 = \{\pm\frac{1}{2}, \pm\frac{1}{2}i, \pm\frac{1}{2}j, \pm\frac{1}{2}k, \frac{1}{4}(\pm 1 + \pm i + \pm j + \pm k)\}. \tag{3.1}$$

We define a second set  $T_2$ :

$$T_2 = \{\frac{1}{2}(\pm 1 \pm i), \frac{1}{2}(\pm 1 \pm j), \frac{1}{2}(\pm 1 \pm k), \frac{1}{2}(\pm i \pm j), \frac{1}{2}(\pm i \pm k), \frac{1}{2}(\pm j \pm k)\}. \tag{3.2}$$

The set  $T_2$  is obtained from left multiplication of  $T_1$  by the quaternion  $1 + i$ . Taken as points on  $S^3$  it forms a  $\{3, 4, 3\}$  dual to the  $T_1$  one. Now it is easy to verify that the Gosset polytope 240 vertices belong to the ten sets:

$$\begin{aligned} S_1 &= (T_2, 0) & S_2 &= (0, T_2) & S_{3,4} &= (T_1, \pm T_1) \\ S_{5,6} &= (T_1, \pm iT_1) & S_{7,8} &= (T_1, \pm jT_1) & S_{9,10} &= (T_1, \pm kT_1). \end{aligned} \tag{3.3}$$

This notation should be interpreted as follows. When two numbers appear as subscripts, the first one (respectively second one) refers to the sign plus (respectively minus) in the next term. Now such a term means that one takes pairs of equal quaternions in  $T_1$ , the second one being subsequently multiplied on the left by the specified unit. The pair of quaternions  $(q_1, q_2)$  finally refers to the point in  $R^8$ .

Now, looking to the ten sets  $S_i$  and the definition of the Hopf map as given in appendix B, it is clear that the 24 vertices in each set give the same value  $Q = q_1 q_2^{-1}$  and therefore belong to the same  $S^3$  fibre of the Hopf bundle. The ten  $Q$  values are  $(\infty, 0, \pm 1, \pm i, \pm j, \pm k)$  and the corresponding points on the base  $S^4$  are given by the permutations of  $(\pm 1, 0, 0, 0, 0)$ , which form a cross polytope in  $R^5$ . In each fibre, the 24 points form a  $\{3, 4, 3\}$  polytope. Note that we could proceed again, using the more familiar Hopf bundle of  $S^3$  with fibres  $S^1$  and base  $S^2$ , and fibre each  $\{3, 4, 3\}$  with six great circles passing through four points each (Manton 1987). The six points on the base  $S^2$  again form a cross polytope (here an octahedron), which gives a nice symmetrical pattern for the whole system.

In addition, each  $\{3, 4, 3\}$  fibre of the Gosset polytope generates a  $\{3, 3, 4, 3\}$  4D sublattice of E8. There are ten such equivalent sublattices passing through the origin, labelled by the ten points on the base  $S^4$ . Let us consider now the point  $P$  in the base  $S^4$  with coordinates  $\frac{1}{\sqrt{5}}(1, 1, 1, 1, 1)$ . It is equidistant to five of the ten base space vertices of the Gosset polytope.  $P$  uniquely defines a 4D space  $E$ . Mapping the Gosset polytope onto  $E$  produces five  $\{3, 4, 3\}$  on the same spherical shell, the remaining five being on a smaller shell. Each set of five  $\{3, 4, 3\}$  forms a  $\{3, 3, 5\}$  icosahedral polytope, and the map of the Gosset polytope onto  $E$  therefore leads to two concentric  $\{3, 3, 5\}$ . This is exactly what is given by Elser and Sloane (1987) in their generation of the icosahedral quasicrystal from E8. So  $E$ , defined by  $P$  on  $S^4$ , is the 'physical space'. The 'orthogonal space'  $E'$  corresponds to the point  $P'$ , opposite to  $P$  on  $S^4$ .

In the following, be careful not to confuse the Hopf map (H-map) (from a  $S^7$  shell in  $R^8$  onto a  $S^4$  basis) and the orthogonal map (O-map) from  $R^8$  onto the quasicrystal 'physical space' in  $R^4$

#### 4. Shell-by-shell construction of the quasicrystal

##### 4.1. Successive shells in E8

We now consider vertices on successive shells around an E8 vertex. The number of vertices on the  $N$ th shell is given by (Conway and Sloane 1988)

$$V_N = 240 \sum_{d|j} d^3 \tag{4.1}$$

where  $d$  runs through all integers dividing  $j$ . Table 1 displays these values for the first shells. Note that the square radius of a shell is half the shell number.

With a shell embedded in a  $\mathcal{P}D$  sphere, the set of vertices on a shell can be split into subsets belonging to  $S^3$  fibres, as for the Gosset polytope. Each fibre H-maps onto a point on the base  $S^4$ . With the H-map as defined in appendix B, it is interesting to consider two orientations of the E8 lattice. The first one, which we call the C (for 'crystallographic') orientation, coincides with the coordinates (2.2) or (2.3) already given. For the second one, the Q (for 'quasicrystalline') orientation, we rotate the above coordinates in such a way that the 4D plane which H-maps onto  $P$

**Table 1.** Number of vertices on shells around the origin of the E8 lattice. The first shell is the Gosset polytope in eight dimensions. See (4.1).

<i>N</i>	Square radius $r^2$	Number of vertices on a shell in E8
1	1/2	240
2	1	2160
3	3/2	6720
4	2	17 520
5	5/2	30 240
6	3	60 480
7	7/2	82 560
8	4	140 400
9	9/2	181 680
10	5	272 160

(section 3) is now H-mapped onto the point (1, 0, 0, 0, 0) on  $S^4$ . This is done by the following  $2 \times 2$  quaternionic matrix  $\mathcal{M}$  acting on pairs of quaternions (points in  $R^8$ ):

$$\mathcal{M} = \begin{pmatrix} \cos \omega & -\sin \omega p' \\ \sin \omega \bar{p}' & \cos \omega \end{pmatrix} \tag{4.2}$$

where

$$\omega = \frac{1}{2} \cos^{-1} 1/\sqrt{5} \quad \text{and} \quad p' = \frac{1}{2}(1 + i + j + k).$$

Note that  $\omega$  and  $p'$  are related to  $P$  as follows. Let  $p$  be the stereographic map onto  $R^4$  of the point  $P$  (on  $S^4$ ). Then  $p = p' \tan \omega$ .  $\mathcal{M}$  acts on a pair  $(q_1, q_2)$  to give the pair  $(q'_1, q'_2)$ . In terms of the cut and projection method,  $q'_1$  is the coordinate in the perpendicular space  $E'$ , while  $q'_2$  is the coordinate in the parallel ('physical') space  $E$ .

*4.2. The base of the fibration in the C orientation*

Let us consider the vertices on the  $N$ th shell surrounding the origin in E8. The radius  $r$  of this shell is  $r = \sqrt{N/2}$ . We first show that, for this  $N$ th shell in E8, the coordinates of the base points take the simple form

$$x_i = \nu_i / N \quad \text{with} \quad \nu_i \in \mathbb{Z}. \tag{4.3}$$

Indeed, consider the first coordinate  $x_0$  on the base. A point  $(q_1, q_2)$  is H-mapped onto  $S^4$  such that

$$x_0 = \cos 2\Omega = \frac{q_2 \bar{q}_2 - q_1 \bar{q}_1}{r^2} = 2 \frac{q_2 \bar{q}_2 - q_1 \bar{q}_1}{N}. \tag{4.4}$$

Since  $r^2 = q_1 \bar{q}_1 + q_2 \bar{q}_2$  it is easy to show that relation (4.3) is satisfied whenever  $4q_2 \bar{q}_2$  is an integer. This is true, as can be seen by inspection of the E8 coordinates given in (2.1). The demonstration for the other  $x_i$  follows from considerations of symmetry. The E8 point group coincides with that of the Gosset polytope. We have seen that the H-map of the Gosset polytope gives a cross polytope on  $S^4$ . Therefore the H-map of any E8 shell shares the cross polytope symmetry. In particular, this symmetry allows permutations of the coordinate axes. Since the base  $S^4$  has unit radius, it follows that

$$N^2 = \nu_0^2 + \nu_1^2 + \nu_2^2 + \nu_3^2 + \nu_4^2. \tag{4.5}$$

It can be shown that any combination of  $\nu_i$  satisfying (4.5) corresponds to a fibre in the  $N$ th shell of E8. This is not a trivial result, but is the consequence of the

elaborate solution of a more general number theory problem (Louck and Metropolis 1981 pp 138–71). This allows the number of base points (e.g. of  $S^3$  fibres) for each shell (see table 2) to be easily enumerated. Indeed, for each shell  $N$ , let us multiply the coordinates on the base by  $N$ . Thus the base points are sent onto a shell of radius  $N$  in the 5D  $Z^5$  lattice (note that it has shell number  $N^2$  in  $Z^5$ ). The number  $c$  of points on a shell in  $Z^5$  is given by Hardy (1920) and simplifies, when the radius is an integer  $N$ , to

$$c(N) = \sum_{q|N} \beta(q) \tag{4.6a}$$

where  $q$  runs through all the divisors of  $N$  and

$$\beta(q) = 10q^3 \left( 1 - \sum_{\text{odd } d|q} \frac{1}{d^2} \right) \tag{4.6b}$$

where  $d$  are odd divisors of  $q$  and  $d < q$ .

**Table 2.** Coordinates of points on the base (with all possible permutations) for the ten first shells. The number  $M$  characterizes the ‘upper’ strata and is related by (4.8b) to the shell number  $N$ . These coordinates are solutions of two diophantine equations (6.1) and could be obtained from the Louck and Metropolis iterative method.

$N$	$M$	$(\nu_0, \nu_1, \nu_2, \nu_3, \nu_4)$
1	1	(10000)
2	4	(11110)
3	5	(22100)
4	8	(22220) (32111)
5	11	(32222)
6	12	(33330) (43311)
7	15	(44322)
8	16	(44440) (55321) (63331) (64222)
9	19	(64432)
10	22	(55543)

### 4.3. The base of the fibration in the Q orientation

Applying the matrix  $M$  to the E8 lattice brings it to what we have called the Q orientation. The structure of the fibration is conserved under this rigid motion, as can be easily verified by applying the map  $h_1$  (appendix B) to a rotated point. The mapped point on  $R^4$  only depends upon  $q_1 q_2^{-1}$ , the invariant quantity associated with a fibre. This means that the base of the fibration in the Q orientation is simply a rotation of the base in the C orientation, such that the point  $\frac{1}{\sqrt{5}}(1, 1, 1, 1, 1)$  of the base  $S^4$  is brought onto the point  $(1, 0, 0, 0, 0)$ .

Now the striking point is that, for each shell, the set of base points are gathered onto ‘horizontal’  $S^3$  small spheres (defined by constant  $x_0$ ), numbered by  $m$  and such that (appendix C)

$$x_0 = n/N\sqrt{5} \tag{4.7}$$

where  $n = 2m$  ( $N$  even) or  $n = 2m + 1$  ( $N$  odd)  $n$  taking integer values between  $M$  and  $-M$ , with

$$M = 2 \lfloor \frac{1}{2}(N\sqrt{5}) \rfloor \quad (N \text{ even}) \quad \text{or} \quad M = 2 \lfloor \frac{1}{2}(N\sqrt{5} + 1) \rfloor \quad (N \text{ odd}) \tag{4.8a}$$



where  $[x]$  means the integer part of  $x$ . Simple arithmetic gives the following unique form to  $M$

$$M = 2[N\tau] - N \quad \text{with } \tau = \frac{1}{2}(1 + \sqrt{5}) \quad \text{the golden ratio.} \quad (4.8b)$$

Each ‘horizontal’ set corresponds to E8 vertices which are 0-mapped onto a single shell in the parallel and perpendicular spaces  $E$  and  $E'$ . Let us call  $\rho$  and  $\rho'$  the corresponding shell radii. As said above,  $\rho$  (respectively  $\rho'$ ) is the norm of  $q'_2$  (respectively  $q'_1$ ). It is easy to establish the relations between  $\rho$ ,  $\rho'$  and the  $x_0$  coordinate on the base  $S^4$  of the fibration:

$$\rho^2 = \frac{1}{2}r^2(1 + x_0) \quad \rho'^2 = \frac{1}{2}r^2(1 - x_0) \quad (4.9)$$

and, since the E8 shell number  $N = 2r^2$ ,

$$\rho^2 = \frac{5N + n\sqrt{5}}{20} \quad \rho'^2 = \frac{5N - n\sqrt{5}}{20} \quad (4.10)$$

where  $n = 2m$  or  $n = 2m + 1$  whenever  $N$  is even or odd.

These shells in  $E$  and  $E'$  are polytopes sharing the  $\{3, 3, 5\}$  symmetry group. It can be a  $\{3, 3, 5\}$ , a  $\{5, 3, 3\}$  or any decorated version of these two polytopes. We now need to decide which shells are to be kept in order to generate the 4D quasicrystal.

#### 4.4. The acceptance domain in the perpendicular space

In the cut and projection scheme, a point in the higher-dimensional lattice is selected whenever its projection onto the perpendicular space  $E'$  falls inside the so called ‘acceptance domain’ (AD). Here (see figure 1), as in Elser and Sloane (1987), we first take as AD the mapping of the Voronoi domain of E8. It is the convex hull of  $\{3, 3, 5\}$  (with radius  $R_{AD} = a/2$ ) and a  $\{5, 3, 3\}$  (with radius  $R'_{AD} = \sqrt{2}a/3$ ), where  $a = ((5 + 2\sqrt{5})/10)^{1/2}$ .

For reasons of symmetry, whenever a point is selected, the whole fibre to which it belongs is also selected. Moreover, and except for the cases discussed below, the above ‘horizontal’ shells (made of fibres sharing the same  $x_0$  value) are kept or immediately rejected. This statement is exact when the AD is a spherical  $S^3$  shell in  $E'$ . Here some care must be taken for shells whose radii fall in between  $R_{AD}$  and  $R'_{AD}$ . For a given E8 shell, and according to equation (4.10), the smallest  $\rho'$  value occurs whenever  $n$  is maximum,  $n = M$  (equation (4.8)). It corresponds to

$$\rho'^2 = (\sqrt{5}/10)(N\tau - [N\tau]) \quad (4.11)$$

which is always smaller than  $R_{AD}^2$ . So, for a given E8 shell, whenever the smaller shell 0-mapped onto  $E'$  is a  $\{3, 3, 5\}$ , it is always selected. Otherwise it could be rejected. However a precise inspection (up to the 20th E8 shell) shows that, for each E8 shell, there is always a small shell in  $E'$  (which means the largest shell in the physical space  $E$ ) which is selected. The difficult cases occur when  $N$  is a Fibonacci number, for which  $\rho'$  comes close to  $R_{AD}$  or  $R'_{AD}$ .

In order to simplify the discussion we can decide to take, as the AD, the  $S^3$  sphere whose radius  $\sqrt{5}/10$  is in between  $R_{AD}$  and  $R'_{AD}$ . This radius is such that, for each E8 shell, exactly one small shell in  $E'$  is selected. The overall symmetry of the selected points in  $E$  (the  $\{3, 3, 5\}$  symmetry) is unchanged. The only difference might be some shells added or subtracted compared with the above Voronoi mapped AD, although this was not found up to the 20th shell (which already amounts to a large cluster).

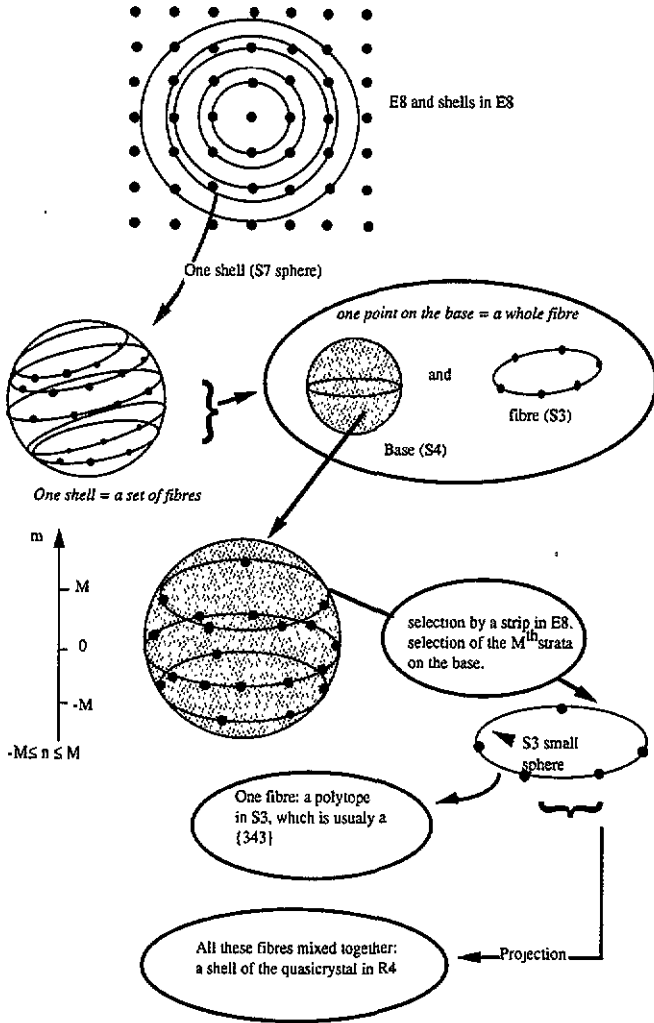


Figure 1. This is a schematic drawing of the method: choose a shell in E8; describe it using fibration; select all fibres corresponding to the strata  $M$ ; mapping on  $R^4$  gives the shell of the quasicrystal.

### 5. The 2D-1D aspect of the shell-by-shell construction

There are two characteristic features of the 4D quasicrystal which are related to the 2D-1D construction of a Fibonacci quasiperiodic chain:

(i) all the shells which contain a common subset of points, up to rescaling, have their radius in one-to-one correspondence with the abscissa of points in a Fibonacci chain.

(ii) if we consider all the shells, whatever their type is, their squared radii also form a Fibonacci chain.

In order to explain the former property, let us first consider  $\{3, 3, 5\}$  shells in the 4D quasicrystal. The first shell in E8 (the Gosset polytope) projects onto two concentric  $\{3, 3, 5\}$  in  $R^4$ , scaled by a factor  $\tau$ . Call  $A_1$  (respectively  $A_2$ ) the star of 120 vectors in  $E$  which point to the vertices of the smallest (respectively the largest)  $\{3, 3, 5\}$ .  $A_1$  generates the whole module obtained by mapping E8. Note that this set

is not minimal.

Consider two vertices, one on each such polytope, which are equivalent under the  $\tau$  scaling. They define two vectors in  $R^4$ ,  $u_1$  and  $u_2$ . When lifted into E8 these two vectors give two orthogonal vectors. Indeed, they belong to two completely orthogonal 4-planes characterized by two opposed points on the base  $S^4$  of the Hopf fibration. These two orthogonal vectors in E8 span a sub-lattice in E8, which is a square lattice, embedded in a 2-plane  $\Pi$ . The physical space  $E$  intersects  $\Pi$  along a straight line  $L$  containing  $u_1$  and  $u_2$ . E8 points belonging to  $\Pi$  and selected by the cut and projection algorithm could be directly selected by the standard 2D-1D algorithm in  $\Pi$ . These points generate a Fibonacci chain in  $L$ . Consequently the radii of the successive  $\{3, 3, 5\}$  shells follow this Fibonacci sequence.

The discussion proceeds along similar lines as for the other types of shells in the 4D quasicrystal. Indeed, consider, for a given type of shell, the one of smaller radius, and select a vector joining the origin to one of its vertex. This vector can be written as a linear combination of vectors in  $A_1$ . The same linear combination, but with the corresponding vectors in  $A_2$ , defines a new vector scaled by  $\tau$ . As in the above discussion, these two vectors are mapped from two orthogonal vectors in E8, which again span a square sub-lattice in E8, embedded in a 2-plane  $\Pi'$ . For the same reason, and because the AD size in this square lattice is in the module of  $(1, \tau)$ , a Fibonacci sequence of the given type of shell will be selected.

The other 2D-1D interesting aspect of the 4D quasicrystal concerns the whole sequence of shells, whatever their type. The surprising result is that, when plotted against their square radius, they display a Fibonacci sequence. The shells' square radius in the quasicrystal space  $E$  and in the orthogonal space  $E'$  read as

$$\rho^2 = (\sqrt{5}/10)(N\tau^{-1} + \lfloor N\tau \rfloor) \quad (5.1)$$

$$\rho'^2 = (\sqrt{5}/10)(N\tau - \lfloor N\tau \rfloor). \quad (5.2)$$

From these relations one recovers without difficulty that the shells' square radii  $\rho^2$  are ordered like a Fibonacci chain. Figure 2 shows this property. The vertical axis corresponds to the shell number  $N$  and the horizontal axis to the number  $n$  associated with different 'horizontal strata' on the base  $S^4$  of the fibration and which is used to label the different shells in  $R^4$  obtained from a single shell in E8. Each point  $(N, n)$  in this figure corresponds to a shell in  $R^4$ . As  $|n| < N\sqrt{5}$ , the whole module, obtained by mapping all the E8 lattice, corresponds to all the points inside the sector  $(n = -N\sqrt{5}, n = N\sqrt{5})$ . The selected shells are those which are represented by points between the two straight lines  $n = N\sqrt{5}$  and  $n = N\sqrt{5} - 2$ . This is obtained when the AD is spherical with a radius  $(\sqrt{5}/10)^{1/2}$ . Recall that the choice of a spherical AD is equivalent to what is obtained using the Voronoi cell as AD: one shell in E8 leads to only one shell in  $R^4$ .

So we again find a construction similar to the 2D-1D construction. But here, all types of shells are concerned, and it is their square radius which follows a quasiperiodic order.

## 6. Toward explicit coordinates for the quasicrystal

### 6.1. The shells on the base of the fibration

The first step for a complete understanding of the quasicrystal shells is a comprehensive description of the points on the basis of the fibration (each such

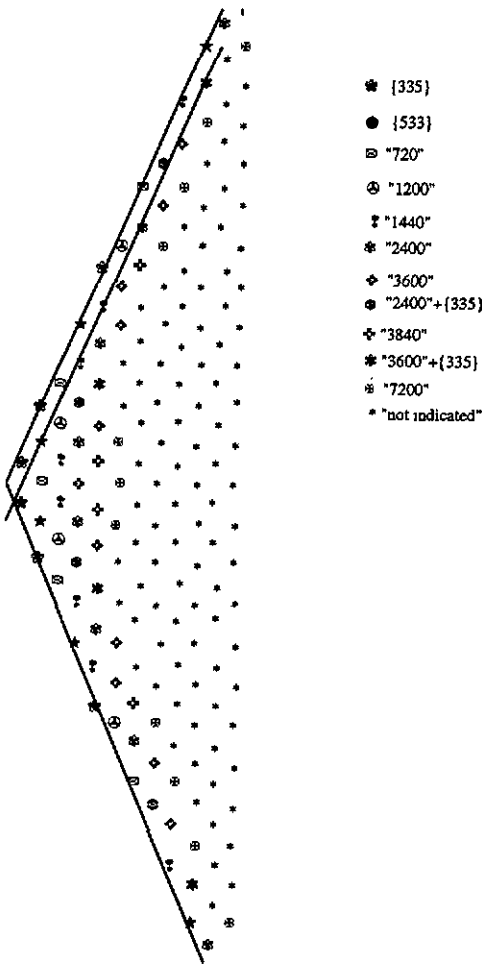


Figure 2. Polytopes are represented by symbols which are plotted on points with coordinates  $(N, n)$ . This figure summarizes table 5. The points, representing polytopes, are inside two lines representing equation  $n = \pm N\sqrt{5}$ . The selected shells correspond to points  $(N, M)$  which are the closest points to the line  $n = N\sqrt{5}$ . Hence they are inside the strip defined by the two parallel lines  $N\sqrt{5}$  and  $N\sqrt{5} - 2$ . This displays the 2D-1D aspect of the shell square radius distribution (5.1).

point corresponding to an  $S^3$  fibre in  $R^8$ ). A quasicrystal shell in  $R^4$  is built from the union of o-mapped fibres, which are such that their H-mapped image belongs to the same  $S^3$  small-sphere of the  $S^4$  base. As explained above, points on the base can also be mapped onto points in the  $Z^5$  lattice. So the selected fibres are given by the intersection of a spherical shell in  $Z^5$  with the reticular  $(1,1,1,1)$  4-plane. Such a 4-plane contains an A4 lattice (Conway and Sloane 1988), and the problem is then to enumerate the successive shells in A4. There is no explicit formula describing these shells, but we can use an iterative method devised by Louck and Metropolis (1981).

With the notation used in section 5, the square radius of the shell in A4 is  $N^2 - n^2/5$ . Whether this shell is centred on an A4 vertex depends upon the value of  $n[5]$ , where  $[5]$  denotes the modulo 5 operation. So we have the following coupled diophantine equations

$$\sum_{i=0,4} \nu_i = M \quad \text{and} \quad \sum_{i=0,4} \nu_i^2 = N^2 \tag{6.1}$$

where  $M$  (the 'strata' number) is given by (4.8b). The Louck and Metropolis algorithm can be summarized as follows.

Define  $R^2 = 5N^2 - M^2$  and  $\chi = -M[5]$ .

Define two integers  $\alpha_{\min} = [R/2]$  and  $\alpha_{\max} = [2R]$  (here  $[x]$  is the first integer

larger than  $x$ ).

Find all integers  $\alpha \in [\alpha_{\min}, \alpha_{\max}]$  such that  $\alpha = -\chi[5]$ .

Now suppose that the multiplet  $\{\nu_i\}$  is ordered in increasing values. Then we have

$$\nu_0 = \frac{1}{3}(M - \alpha). \tag{6.2}$$

The remaining values  $\{\nu_1, \nu_2, \nu_3, \nu_4\}$  are again subject to coupled diophantine equations of the type (6.1) and the algorithm can be used again (but with the number 4 replacing 5). This is easily implemented on a computer, and the first values are given in table 2. Once a multiplet is obtained, new ones are immediately derived by permutations. So the number of fibres on a 'strata' is given by the number of different solutions to (6.1) multiplied by the corresponding number of permutations.

Another interesting property concerns the quantity  $R^2$ .  $R^2$  characterizes a given type of polytopal shell (e.g. all the  $\{3, 3, 5\}$  correspond to  $R^2 = 4$ , the  $\{5, 3, 3\}$  to  $R^2 = 16, \dots$ ). This is true for all the shells in the quasicrystal. This point is developed further in section 6.3.

### 6.2. The corresponding shells in E8

For reasons of symmetry, the fibres whose coordinates are equivalent, up to a permutation, contain the same set of E8 vertices. In most cases it is a  $\{3, 4, 3\}$  polytope (with 24 vertices), but it is sometimes a decorated version of the latter.

Let us first consider the case where the number of points on the base  $S^4$  is  $10 \sum_{q|N} q^3$  (which is a particular case of formula (4.6)) and suppose that there are exactly 24 vertices on each fibre. We then recover the known value  $240 \sum_{q|N} q^3$  (formula (4.1)) for the number of vertices in a E8 shell. So the cases where a fibre contains more than 24 vertices correspond to the corrections to the  $q^3$  term in formula (4.6b). We can rewrite (4.6) in the following way:

$$c(N) = 10 \left( \sum_{q|N} q^3 - \sum_{q|N} \sum_{\substack{d|q \\ \text{odd}, d \neq q}} d \left( \frac{q}{d} \right)^3 \right). \tag{6.3}$$

Since  $q/d$  divides  $N$ , this can be put in the following form

$$c(N) = 10 \left( \sum_{q|N} q^3 \left( 1 - \sum_{\substack{d|(N/q) \\ \text{odd}, d \neq 1}} d \right) \right). \tag{6.4}$$

This allows us to obtain the number of points on each fibre which is explicitly done for the ninth shell in table 3. The corresponding numbers for the first nine shells are given in table 4.

### 6.3. The quasicrystal shells

A shell of the quasicrystal in  $R^4$  is obtained from all the fibres which are represented by points on the highest strata on the base (they are characterized by the two numbers  $N$  and  $M$ ). Recall that  $N$  originally labels E8 shells. But, since for the highest strata on the base,  $M$  is unequivocally derived from  $N$ , then  $N$  also labels a shell in the 4D quasicrystal. These fibres O-mapped onto  $R^4$  lead to a whole shell in the quasicrystal.

If we are interested in the explicit coordinates of vertices in the quasicrystal the procedure comprises a lift of the coordinates on the base toward coordinates in E8. As all points on the same fibre give one point on the base, there is some uncertainty in

**Table 3.** With the example of the ninth shell, this table explains how the number of points on the base (written in standard figures) is related to the number of points on a fibre (in italic figures). The upper numbers are absolute values of the 'strata' numbers for all the strata obtained by mapping the ninth shell in E8 on  $R^4$ . The number of points on the base is given by (6.4) applied to  $N = 9$ :  $c(10) = 10[1^3 \times (1 - 3 - 9) + 3^3 \times (1 - 3) + 9^3]$ . There are  $10(1 + 3^3 + 9^3)$  sets of 24 vertices. Some sets are individual fibres, some others are mixed in fibres containing more than 24 vertices. The first corresponds to what appears in the line labelled no 9, the others in line shell no 1 and shell no 3. These two lines are obtained from the shell number 1 (because there is a correction  $d = 9$  in the term in factor of  $1^3$ , and because  $N/d = 1$ ) and from the shell number 3 ( $d = 3$  correction in  $3^3$  term, and  $N/d = 3$ ). In these two cases the  $n$  numbers are replaced by  $d \cdot n$ , and the number of points on the fibre have a factor  $d$ .

	1	3	5	7	9	11	13	15	17	19
Shell no 1					5					
x9					24 x 9					
Shell no 3		60			5			30		
x3		24 x 3			24 x 4 x 3			24 x 3		
					30					
					24 x 3					
Shell no 9	180120	120120	120240	180120	60120	12060	60120	603030	12030	60
	120	606060	606060	306060	303060	12060	6060	3060		
	24	24	24	24	5	24	24	24	24	24
					24					
Total	24	96 on 60 24 else	24	24	96 on 30 24 x 21 on 5 24 else	24	24	96 on 30 24 else 24 else	24	24

this operation. But if one set of coordinates in E8 which would lead to the considered point on the base can be found, other points on the same shell can be obtained using point group symetries. Then, applying O-mapping leads to the coordinates for the quasicrystal.

In summary we want to determine a set of coordinates in E8 written as two quaternions  $(q_1, q_2)$  with  $q_2 \bar{q}_2 + q_1 \bar{q}_1 = N/2$ . Call  $(\nu_0, \nu_1, \nu_2, \nu_3, \nu_4)$  the five coordinates of the H-mapped point  $(q_1, q_2)$  on the base  $\nu_0 = q_2 \bar{q}_2 - q_1 \bar{q}_1$ . Call  $q_\nu$  the quaternion  $(\nu_1, \nu_2, \nu_3, \nu_4)$ . We have the relation  $(N - \nu_0)q_1 = q_\nu q_2$ .

So the problem is to obtain two possible quaternions  $q_1$  and  $q_2$  compatible both with this relation and with E8 coordinates for a given set of  $\nu_i$ . We do not have a general algorithm which gives explicit coordinates for all vertices of all the quasicrystal shells.

Knowing the number of vertices on each shell of the quasicrystal is another good way to characterize this structure. We now discuss the question of obtaining this number from the shell number  $N$ .

We now suppose that the number  $R^2 = 5N^2 - M^2$  characterizes the type of shell in the quasicrystal. It is clear as a straightforward consequence of Louck and Metropolis (1981) that  $R^2$  characterizes the number of fibres leading to a quasicrystal shell, but the question of the number of vertices on each fibre remains. We have discussed the fact that some fibres have more than 24 vertices: this occurs for the selected one if there is an odd divisor  $p$  of  $N$  (see (6.4)) such that

$$N = pN' \quad \text{and} \quad [N\tau] = p[N'\tau].$$

**Table 4.** Number of vertices for the first nine shells depending on the strata number  $n$  which are odd for odd  $N$ , and even for even  $N$ . The number of points on the base is written in standard figures, with the number of vertices on the fibre (in italic figures); when this number is 24 it is not always written. When these shells in E8 are mapped in the  $E_8$  physical space, polytopes are obtained with a number of vertices which is the number of points on fibres times the number of corresponding fibres. For instance  $5 \times 24 = 120$  for  $N = 1, n = 1$ , which corresponds to the  $\{3, 3, 5\}$  polytope or  $(20 + 5) \times 24 = 600$  for  $N = 1, n = 8$  corresponding to the  $\{5, 3, 3\}$  polytope.

	0	1	2	3	4	5	6	7	8
1		5 24							
2	30 24		20; 5 24		5 24				
3		60 24		5; 30 96; 24		30 24			20; 5 24
4	120; 30 24		100 24		5; 20; 80 24		60 24		
5		20; 20; 120 24		120; 30 24		5; 5; 120 144; 24		20; 20; 60 24	120; 30 24
6	30; 120; 60 96; 24		60; 120; 120 24		60; 150 24		20; 5; 30; 60; 60 96; 24		
7		60; 40; 120; 90 24		60; 60; 60; 120 24		60; 60; 120 : 60; 60		5; 60; 60; 90 192; 24	
8	120; 120; 120 : 240; 90		120; 80; 80; 120		120; 80; 100; 20; 180		180; 180 24		5; 180; 60; 80 20; 60; 20
9		180; 120; 120 : 30; 60		60; 120; 120; 60; 60 96; 24		120; 240; 60 : 60; 60		180; 120; 30 : 60; 60	
5	60 24		5 24						
6		30; 120; 60 24		5; 30 96; 24					
7	60; 120; 30 24		60; 20; 20; 60 24		60; 20; 60 24		30 24		
8		120; 60; 60; 120 24		120; 60; 60; 60		60; 20; 20; 60 24		20; 20; 60; 5 24	
9	30; 60; 120; 30; 60; 5 96; 24; 504		120; 120; 60; 60		120; 60; 120; 60		30; 30; 30; 60; 60 96; 24		120; 30 24 60 24

The second condition indicates that it is the selected fibre which has more than 24 points. These two equations are written as a condition on the  $R^2$  number:

$$R'^2 = 5N'^2 - M'^2 \quad \text{and} \quad R^2 = p^2 R'^2.$$

So if a fibre has a multiple of 24 vertices for a given  $N$ , it occurs, with the same mechanism, for all  $N$  leading for the same  $R^2$  value characterizing a shell of the quasicrystal.

In addition to the  $N$  number, we introduce two other related numbers  $N_+ = \lfloor N\tau \rfloor$  and  $N_- = \lfloor N/\tau \rfloor$ . The three numbers  $N_-$ ,  $N$ ,  $N_+$  are parts of (and define) a Lucas series ( $N_+ = N + N_-$ ). With this notation,

$$R^2 = 5N^2 - (N_- + N_+)^2 \quad \text{or} \quad R^2 = 4(N^2 - N_-^2 - NN_-) \tag{6.5}$$

showing that all  $R^2$  are multiples of 4. A Lucas number  $L_n$  can be written using Fibonacci numbers  $F_n$  (Schroeder 1984),  $L_n = G_1 F_{n-1} + G_2 F_n$  where  $G_1$  and  $G_2$  are integers. A particular case is the Fibonacci numbers obtained with  $G_1 = 0$  and  $G_2 = 1$ . With a little arithmetic, using classical relations for Fibonacci numbers, we have, from  $N = G_1 F_{n-1} + G_2 F_n$ , the result  $R^2 = 4(-G_1^2 + G_2^2 - G_1 G_2)$ . All the Lucas numbers of the same series give  $L_n^2 - L_{n-1}^2 - L_n L_{n-1} = R^2/4$  showing that all the  $N$ , with an index of the same parity in the same Lucas series defined by  $N_-$ ,  $N$ ,  $N_+$ , have the same  $R^2$ , and so they correspond to similar shells in the quasicrystal. There is a restriction to this condition. If a shell number  $N = L_n$  then  $\lfloor N\tau \rfloor = L_{n+1}$  must be true. This condition could exclude some of the first terms of the Lucas series. The simplest example of the relation between Lucas numbers and the type of shell is given by Fibonacci numbers:  $R^2/4 = 1$ . All shells labelled by  $N = 1, 2, 5, 13, \dots$  (which are even Fibonacci numbers  $F_{2n+1}$ ) are similar: they are  $\{3, 3, 5\}$  polytopes. Note here that we stated in section 5 that all  $\{3, 3, 5\}$  polytopes have their radii in correspondence with the abscissa of points in a Fibonacci quasiperiodic chain.  $N = F_{2n+1}$  corresponds to some of these points, but not all. It means that some shells which are not simply  $\{3, 3, 5\}$  polytopes contain a  $\{3, 3, 5\}$  polytope, as a subset, with the same orientation.

The quasiperiodic chain corresponds to all shells which are, or which contain, similar  $\{3, 3, 5\}$  polytopes. The even Fibonacci numbers correspond to purely similar  $\{3, 3, 5\}$  polytopes. This remark extends to all types of shell.

In order to study the possible values for  $R^2/4$ , let us first suppose that  $G_1$  and  $G_2$  are coprimes. The first possible values are given in table 5 with the first  $N$  at which they occur.

Another possibility is that  $G_1 = 0$ . In this case  $N = G_2 F_{2n+1}$ , a multiple of a Fibonacci number, and  $R^2/4 = G_2^2$ . Consequently, all squares are possible values for  $R^2/4$ . Finally, if  $G_1$  and  $G_2$  have a common divisor we get  $G_1 = pG'_1$  and  $G_2 = pG'_2$  with  $R^2/4 = G_2'^2 - G_1'^2 - G'_1 G'_2$  and  $R'^2/4 = p^2 R^2/4$  showing that  $R^2/4$  could be a product of possible different values of other  $R^2/4$ . Table 5 gives, for the first 34 shell, the value of  $R^2/4$ ,  $G_1$ ,  $G_2$  and the number  $\chi$  of vertices on the shell. It appears that the following relation is verified:

$$\chi = 120 \sum_{q|Q} q \tag{6.6}$$

with  $Q = R^2/4$  and where  $q$  are all divisors of  $Q$  including 1 and  $Q$  which are in the set of possible values of  $R^2/4$ . We have no proof of this relation but it has been tested up to the 37th shells, therefore we leave it as a conjecture. Its veracity would be highly valuable as it gives a very simple way to obtain the number of points on a shell in this 4D quasicrystal (nevertheless see Moody and Patera (1993)).



Table 5. The numbers  $R^2$  and  $R^2/4$ , which are characteristic of shells, are given for the first 34 shells. These numbers are obtained from (6.6). The two numbers  $G_1$  and  $G_2$  are the Lucas series generator such that  $N$  belongs to a Lucas series. The relation (6.6) is exemplified in the last two columns.

$N$	$R^2$	$R^2/4$	$G_1$	$G_2$	Number $\chi$ of vertices on shell	Construction of this number/120
1	4	1	0	1	120	1
2	4	1	0	1	120	1
3	20	5	1	3	720	1 + 5
4	16	4	0	2	600	1 + 4
5	4	1	0	1	120	1
6	36	9	0	3	1200	1 + 9
7	20	5	1	3	720	1 + 5
8	64	16	0	4	2520	1 + 16 + 4
9	44	11	1	4	1440	1 + 11
10	16	4	0	2	600	1 + 4
11	76	19	1	5	2400	1 + 19
12	44	11	1	4	1440	1 + 11
13	4	1	0	1	120	1
14	80	20	2	6	3600	1 + 20 + 5 + 4
15	36	9	0	3	1200	1 + 9
16	124	31	2	7	3840	1 + 31
17	76	19	1	5	2400	1 + 19
18	20	5	1	3	720	1 + 5
19	124	31	2	7	3840	1 + 31
20	64	16	0	4	2520	1 + 16 + 4
21	180	45	3	9	7200	1 + 45 + 5 + 9
22	116	29	4	9	3600	1 + 29
23	44	11	1	4	1440	1 + 11
24	176	44	4	10	7200	1 + 44 + 4 + 11
25	100	25	0	5	3720	1 + 25 + 5
26	16	4	2	4	600	1 + 4
27	164	41	5	11	5040	1 + 41
28	76	19	1	5	2400	1 + 19
29	236	59	5	12	7200	1 + 59
30	144	36	0	6	6000	1 + 36 + 9 + 4
31	44	11	2	5	1440	1 + 11
32	220	55	6	13	8640	1 + 55 + 11 + 5
33	116	29	1	6	3600	1 + 29
34	4	1	0	1	120	1

## 7. Quasicrystals of lower dimension

It is possible to obtain a quasicrystal of dimension  $d \leq 3$  by sectioning the 4D quasicrystal with a  $d$ -dimensional plane of high symmetry.

An obvious example is the 1D Fibonacci quasicrystal which appears along straight lines through the origin of the quasilattice in different directions of symmetry related to the  $[3,3,5]$  symmetry group. For instance consider one point on the  $\{3,3,5\}$  polytope which is the first shell of the 4D quasicrystal and the corresponding point of the second shell which is related by a  $\tau$  inflation. These two points aligned with the origin generate a 1D Fibonacci chain.

### 7.1. 3D quasicrystals with icosahedral symmetry

We now discuss some 3D examples. Two-dimensional structures, except the one with

30-fold symmetry, are not presented here but they could be obtained by cutting into the 3D structures.

We look for a 3D plane which must be invariant under a subgroup of the  $[3, 3, 5]$  symmetry group, and we characterize its position relative to the first shell surrounding the origin in the 4D quasicrystal. This  $\{3, 3, 5\}$  polytope is embedded into an  $S^3$  sphere which can be cut by the 3-plane along a  $S^2$  sphere. A particular orientation of the 3-plane is found and selected when it contains vertices of the polytope which form regular or semi-regular polyhedra on this  $S^2$  sphere. It is possible to describe the  $\{3, 3, 5\}$  polytope using concentric spherical  $S^2$  shells in  $S^3$  (Coxeter 1973). Consider a vertex on a pole of  $S^3$ : the first shell is an icosahedron, the second is a dodecahedron, the third a larger icosahedron; the fourth shell, in an equatorial position on a great sphere ( $S^2$ ) of  $S^3$ , is an icosidodecahedron (figure 3). With this orientation of the polytope, all these shells share the icosahedral symmetry and then define a 3-plane containing a quasicrystal which has icosahedral symmetry.

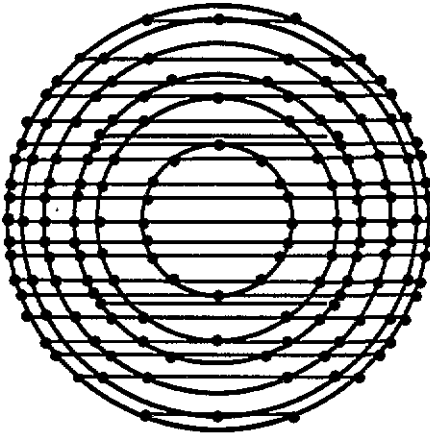


**Figure 3.** The first six shells of the quasicrystal are represented by concentric circles. These shells which are 4D polytopes are oriented such that the first shell which is a  $\{3, 3, 5\}$  polytope has a vertex on a pole and an icosidodecahedron on the equatorial sphere: these two sets of points are represented on the first circle by a horizontal diameter (schematizing the equatorial sphere) and a pole in the orthogonal direction. With this orientation, the  $\{3, 3, 5\}$  could be decomposed, from the pole, into an icosahedron, a dodecahedron, a larger icosahedron, the icosidodecahedron and then symmetrically in the other hemisphere. These polyhedra are represented by horizontal segments terminated by two points on the circle. The other shells are also decomposed into polyhedra (all vertices of a polyhedron have the same fourth coordinate). Consider a 3D cut of the quasicrystal represented by a horizontal line. It contains a 3D quasicrystal with icosahedral symmetry, but with a different structure depending on the fourth coordinate.

First consider the 3-plane through the origin which cuts the  $\{3, 3, 5\}$  along an icosidodecahedron. All its shells are equatorial shells ( $S^2$ ) of successive ( $S^3$ ) shells cut in the 4D quasicrystal. As in the 4D counterpart their square radii form a Fibonacci sequence, and the radius of a given type of shell is found with quasiperiodic order. However, if a 4D shell has no point in the 3D plane it could mean that some shells are missing in the 3D quasicrystal.

It is also possible to consider a 3-plane not through the origin but characterized by another type of polyhedral shell of the  $\{3, 3, 5\}$  polytope, for instance an icosahedron. In this case the 3D quasicrystal does not have a vertex at the origin; its first shell is an

icosahedron, the second shell a dodecahedron, the third shell an icosidodecahedron etc (as explained schematically in figure 3). In this case, the square radii of the successive shells are not organized as a Fibonacci chain but equal  $r_i^2 + \frac{1}{4}\tau^2$  (where  $r_i^2$  is in units of the first shell radius in the 4D quasicrystal). So there are numerous possibilities for 3D quasicrystals with icosahedral symmetry using different choices of 3D planes, possibly with some thickness.

### 7.2. 3D quasicrystals with tetrahedral symmetry

The  $\{3, 3, 5\}$  polytope has other symmetry subgroups; an interesting example is the tetrahedral symmetry. Consider a  $\{3, 3, 5\}$  polytope oriented such that the centre of a cell is at a pole. Then the successive shells are: a tetrahedron, another tetrahedron inflated by  $\tau$ , an octahedron, two shells with 12 vertices located on the edges of a cube (some faces are golden rectangles), another tetrahedron inflated by  $\tau^2$  and finally a cuboctahedron on the equatorial sphere. If we consider the 3D plane through the origin, containing this cuboctahedron, it contains a quasicrystal with a tetrahedral symmetry (and even maybe of octahedral symmetry, this should be checked). Note that the first shell is the same as in an FCC close packed structure.

### 7.3. A 2D quasicrystal with 30-fold symmetry

Finally let us consider a particular case in two dimensions: a quasicrystal with 30-fold symmetry. It is known from group theory arguments that such point symmetry could be obtained by mapping from a lattice in eight dimensions. Indeed there are eight integers lower and coprime to 30. The E8 point group has a subgroup isomorphic to the  $[3, 3, 5]$  symmetry group. The latter contains 30-fold 'screw' symmetry axes (Coxeter 1973). In the  $\{3, 3, 5\}$  polytope, the orbits under this symmetry are screw polygons wrapped onto a torus embedded in  $R^4$ . When mapped onto the two orthogonal symmetry planes, they appear as either a 30-fold regular polygon or a 30/11 star polygon. Therefore, choosing one of these two planes as 'physical space', we can generate a 2D 30-fold quasicrystal. However, it is not a simple cut of the 4D quasicrystal. One needs, as in the usual cut and projection method, to select points located close to the physical space. More precisely, the AD in the orthogonal plane can be any polygon of finite radius, whose symmetry is a multiple of 30 (or even a circle as limit case).

## Appendix A. Quaternions

A quaternion  $q$  is given by

$$q = q_0 + q_1i + q_2j + q_3k \quad q_0, q_1, q_2, q_3 \in \mathbb{R} \quad (\text{A1})$$

with  $i^2 = j^2 = k^2 = ijk = -1$  the latter 'Hamilton' relations defining the multiplication rules which are non-commutative. Quaternions, which form a corpus  $H$ , can also be viewed as ordered pairs of complex numbers with the following rules for addition and multiplication:

$$\begin{aligned} (s, t) + (u, v) &= (s + u, t + v) \\ (s, t)(u, v) &= (su - t\bar{v}, sv + t\bar{u}) \end{aligned} \quad (\text{A2})$$

where  $s, u, v, t \in \mathbb{C}$  and  $\bar{u}$  is the complex conjugate of  $u$ . The quaternion conjugate is defined as

$$\bar{q} = q_0 - q_1i - q_2j - q_3k. \quad (\text{A3})$$

Also the norm  $N_q$  is such that

$$N_q^2 = q\bar{q} = \sum_{i=1}^4 q_i^2 \geq 0. \tag{A4}$$

There is another way in which  $q$  can be written as a scalar part  $S(q)$  and a vector  $V(q)$ :

$$q = S(q) + V(q) \quad S(q) = q_0 \quad V(q) = q_1i + q_2j + q_3k \tag{A5}$$

with the relations

$$S(q) = \frac{1}{2}(q + \bar{q}) \quad V(q) = \frac{1}{2}(q - \bar{q}). \tag{A6}$$

A quaternion is said to be real if  $V_q = 0$  and pure imaginary if  $S_q = 0$ . We shall also write  $V_i(q)$  to denote the component of  $V(q)$  along  $i$ . Let  $Q$  be the set of unit norm quaternions. It is a non-commutative group isomorphic to  $SU(2)$  and to  $S^3$  (considered as a topological group). A quaternion in  $Q$  can be written

$$q = \cos \alpha + y \sin \alpha \quad \text{or} \quad q = \exp \alpha y \tag{A7}$$

where  $y$  is a pure imaginary quaternion. Remember that quaternion multiplication is not commutative so

$$\exp(\alpha y) \exp(\beta z) = \exp(\alpha y + \beta z) \tag{A8}$$

only if  $y = z$ .

Of interest in the present work is the group of integral unit quaternions  $T$ , sometimes called the Hurwitz group, or the binary tetrahedral group. It contains the following 24 elements

$$T = \{\pm 1, \pm i, \pm j, \pm k, \frac{1}{2}(\pm 1 + \pm i + \pm j + \pm k)\} \tag{A9}$$

If one considers the group elements as points on the unit sphere  $S^3$ , they form a  $\{3, 4, 3\}$  self-dual polytope. Note that the set of vertices of the  $\{3, 3, 4, 3\}$  tessellation, taken as vectors, form a ring whose units are precisely the elements of  $T$  (du Val 1964). Quaternions can also be used in eight dimensions, with points described as pairs of quaternions.

### Appendix B. The Hopf map

There are two well known Hopf fibrations of (high-dimensional) spheres by (lower-dimensional) spheres. The most famous is the fibration of  $S^3$  by great circles  $S^1$  and base  $S^2$ . It is non-trivial ( $S^3 \neq S^2 \times S^1$ ). This fibration can be extended to the whole  $R^4$  as a bundle of 2-planes which only meet at the origin. The second fibration, that of  $S^7$  with fibres  $S^3$  and base  $S^4$ , is used in this paper in a discretized form.

A point on the sphere  $S^7$  has its coordinates given by a pair of quaternions  $(q_1, q_2)$  subject to  $q_1\bar{q}_1 + q_2\bar{q}_2 = 1$ .  $S^7$  can be fibred such that the quaternion  $Q = q_1q_2^{-1}$  is invariant on each fibre  $S^3$ , and therefore uniquely specifies the fibre.  $Q$  can be any quaternion, including  $\infty$ , which shows that the base space of the bundle is  $S^4$ . The latter can be viewed as the inverse stereographic projection from  $R^4$  to  $S^4$ . In this paper we shall define fibrations on  $S^7$  with different radii  $r$ , with an attempt to compare the results on the base  $S^4$  (or, equivalently, to compare the  $Q$  values). In doing so, one should take care of rescaling each  $S^7$  to a unit radius  $S^7$ . In term of coordinates, the H-map can be written as the composition of the map  $h_1$  from  $S^7$

to  $R^4$  (with  $\infty$  included) followed by an inverse stereographic projection from  $R^4$  to  $S^4$ :

$$\begin{aligned}
 h_1: \quad S^7 &\longrightarrow R^4 \\
 (q_1, q_2) &\longrightarrow Q = q_1 q_2^{-1} \quad q_1, q_2 \in H \\
 h_2: \quad R^4 &\longrightarrow S^4 \\
 Q &\longrightarrow M = (x_0, x_1, x_2, x_3, x_4) \quad x_i \in \mathbb{R}.
 \end{aligned}
 \tag{B1}$$

The coordinates on  $S^4$  read

$$\begin{aligned}
 x_0 &= \cos 2\Omega \\
 x_1 &= \sin 2\Omega S(Q') \\
 x_2 &= \sin 2\Omega V_i(Q') \\
 x_3 &= \sin 2\Omega V_j(Q') \\
 x_4 &= \sin 2\Omega V_k(Q')
 \end{aligned}
 \tag{B2}$$

where  $Q = N_Q Q'$ ,  $N_{Q'} = 1$ ,  $\Omega = \tan^{-1} N_Q / r$ . Recall that the  $V_i(q)$  denote the component of  $V(q)$  along  $i$  (appendix A). Note that, as for the first H-map, this fibration can be extended to the whole  $R^8$  as a bundle of 4-planes which only meet at the origin. Let us now come to the discretized Hopf fibrations. We have already used such concepts for the  $S^3$  Hopf fibration in the context of polytope models of amorphous solids (Nicolis *et al* 1986, 1988). If we are interested only in the geometry of a discrete set on  $S^7$  (a polytope), we can restrict ourselves to a finite set of  $S^3$  fibres, each containing a discrete set of points. When the set on  $S^7$  is highly symmetrical, it is possible to choose the orientation of the discrete bundle so that each of the  $S^3$  fibre contains a symmetrical set, the base  $S^4$  also showing a symmetrical pattern. For example, as explicitly described by Manton (1987), the 240 vertex Gosset polytope on  $S^7$  is fibred into ten discretized  $S^3$  with 24 vertices each (forming a  $\{3, 4, 3\}$  polytope, the base having ten points forming a cross polytope—see section 3).

**Appendix C**

Let us consider for each shell in E8 the corresponding unit radius  $S^4$  base. If it is in the Q orientation, the  $x_0$  coordinate for each fibre is just the scalar product of the corresponding vector in the C orientation with the vector  $1/\sqrt{5}(1, 1, 1, 1, 1)$ . Therefore, if the coordinates in the C orientation are  $\{\nu_i/N\}$ , the new  $x_0$  simply reads

$$x_0 = \sum_{i=0}^4 \nu_i / N\sqrt{5}.
 \tag{C1}$$

Since  $\sum \nu_i^2 = N^2$  and  $\sum \nu_i$  has the same parity as  $\sum \nu_i^2$ , we recover equation (4.7). Going back to the representations of the  $S^4$  bases as shells with integer radii in  $Z^5$  (section 4.2), the above slicing of  $S^4$  into small  $S^3$  spheres amounts to take the intersections of the  $Z^5$  shells with the successive reticular 4D lattices with Miller indices (1,1,1,1,1). The interspacing in this reticular family is  $1/\sqrt{5}$ . Each 4-plane in

intersection is  $2/\sqrt{5}$  which gives, once normalized, the value  $2/N\sqrt{5}$  as expected from equation (4.7).

In order that  $x_0$  remains  $\leq 1$ , we have

$$\frac{2m}{N\sqrt{5}} \leq 1 \quad N \text{ even} \quad \text{or} \quad \frac{2m+1}{N\sqrt{5}} \leq 1 \quad N \text{ odd} \quad (\text{C2})$$

which gives the  $M$  values of equation (4.8). The fact that  $m$  takes all possible values between  $-M$  and  $M$  is more subtle but can be proved (Louck and Metropolis 1981 pp 138–71).

Let us just have a simple insight into this problem. We have

$$\sum \nu_i = n \quad \text{and} \quad \sum \nu_i^2 = N^2. \quad (\text{C3})$$

We can prove first that, for each  $N$  and for each integer  $p \leq N$ , there is a set  $\nu_i$  such that one of the  $\nu_i$  equals  $p$ . Indeed, suppose that  $\nu_0 = p$ . Then conditions (C3) would imply that

$$\sum_{i=1}^4 \nu_i^2 = N^2 - p^2. \quad (\text{C4})$$

Since any number can be written as a sum of four squares (Hardy and Wright 1968), it is always possible to fulfil condition (C4). Now change  $p$  into  $-p$ . This decreases  $\sum \nu_i$  by  $-2p$ . So there are  $N$  sets  $\nu_i$  (not necessarily different), such that new sets, with one  $\nu_i = p$ , ( $p \leq N$ ) of the opposite sign, can be generated which fulfil equations (C3), but with the sum of the coordinates decreased by  $2p$ . So we see how new values of  $m$  can be obtained, but this does not yet prove that all values of  $m$  are reached.

## References

- Baake M, Joseph D, Kramer P and Schlottmann M 1990 *J. Phys. A: Math. Gen.* **23** L1037  
 Conway and Sloane 1988 *Sphere Packings, Lattices and Groups* (Berlin: Springer)  
 Coxeter H S M 1973 *Regular Polytopes* (New York: Dover)  
 Duneau M and Katz A 1985 *Phys. Rev. Lett.* **54** 5688  
 du Val 1964 *Homographies, Quaternions and Rotations* (Oxford: Oxford University Press)  
 Elser V 1985 *Phys. Rev. B* **32** 4982  
 Elser V and Sloane 1987 *J. Phys. A: Math. Gen.* **20** 6161  
 Hardy G H 1920 *Trans. Am. Math. Soc.* **21** 255  
 Hardy G H and Wright E M 1968 *An Introduction to the Theory of Numbers* (Oxford: Oxford University Press)  
 Kalugin P A, Kitaev A Y and Levitov L C 1985a *JETP Lett.* **41** 145  
 — 1985b *J. Physique Lett.* **46** L601  
 Louck J D and Metropolis N 1981 *Adv. Appl. Math.* **2** 138–71  
 Manton N S 1987 *Commun. Math. Phys.* **113** 341–51  
 Moody R V and Patera J 1993 *J. Math. Phys.* submitted  
 Mosseri R and Sadoc J-F 1984 *J. Physique Lett.* **L827**  
 Nicolis S, Mosseri R and Sadoc J-F 1986 *Europhys. Lett.* **2** 157  
 — 1988 *J. Physique* **49** 599  
 Sadoc J-F and Mosseri R 1988 *Quasicrystalline Materials: ILL-CODEST Workshop* ed C Janot and J-M Dubois (Singapore: World Scientific) pp 215–23  
 — 1990 *J. Physique* **51** 205  
 Schroeder M R 1984 *Number Theory in Science and Communications* (Berlin: Springer)